The stratigraphic record of changing hyperaridity in the Atacama Desert over the last 10 Ma

Alberto Sáez[1*]; Lluís Cabrera[1]; Miguel Garcés[1], Paul van den Bogaard[2], Arturo Jensen[3], Domingo Gimeno[4]

[1] Departament d'Estratigrafia, Paleontologia i Geociencies Marines, Grup de Geodinàmica i Anàlisi de Conques, Universitat de Barcelona, Spain. *Corresponding author: a.saez@ub.edu

[2] GEOMAR | Helmholtz Centre for Ocean Research Kiel, Germany

[3] Departamento de Ciencias Geológicas. Universidad Católica del Norte. Antofagasta, Chile.

[4] Departament de Geoquímica, Petrologia i Prospecció Geológica. Universitat de Barcelona, Spain.

ABSTRACT

New radiometric and magnetostratigraphic data from Quillagua and Calama basins (Atacama Desert) indicate that the stratigraphic record over the last 10 Ma includes two hiatuses, lasting approximately 2 and 4 million years respectively. These sedimentary gaps are thought to represent prolonged periods of hyperaridity in the region, with absence of sediment production and accumulation in the central depressions. Their remarkable synchrony with Antarctic and Patagonian glacial stages, Humboldt cold current enhancement and cold upwelling waters lead us to suggest long-term climate forcing. Higher frequency climate (orbital precession and eccentricity) forcing is thought to control the sequential arrangement of the lacustrine units deposited at times of lower aridity. Hyperaridity trends appear to be modulated by the activity of the South American Summer Monsoon, which drives precipitation along the high altitude areas to the east of Atacama. This precipitation increase combined with the eastward enlargement of the regional drainage during the late Pleistocene enabled water transfer from these high altitude areas to the low lying closed Quillagua basin and resulted in the deposition of the last widespread saline lacustrine deposits in this depression, before its drainage was open to the Pacific Ocean.

Keywords: Late Neogene, Antarctic and Patagonian Glaciations, Humboldt Current, South American Summer Monsoon, hyperaridity.

1. Introduction

The Atacama Desert has existed for approximately 15 million years (Hartley and Chong, 2002; Le Roux, 2012). This subtropical hyperarid desert is of great geologic interest because its climatic evolution has been

controlled by two major tectonic and paleoceanographic forces such as: (1) the uplift of the Central Andes with its Atlantic rain shadow effect; and (2) the intensity of the cold water advection fed by the Humboldt Current and its control on the temperature of the coastal upwelling water that modulates the strength of the subtropical anticyclone. The east-west sea surface temperature contrast over the SE Pacific would be finally the most significant factor leading to more or less hyperaridity (Garreaud et al., 2010 and references therein). In addition, the water balance in Atacama is found to be modulated at higher frequency time scales by the South American Summer Monsoon (SASM) that contributes with precipitation along the higher altitude areas that fringe the eastern margins of the region (Betancourt et al., 2000).

Climatic studies of the Late Cenozoic of the Atacama region have been focused on establishing the age and driving mechanism leading to hyperarid conditions (Gaupp et al., 1999; Hartley and Chong, 2002; Hartley, 2003; Dunai et al., 2005; Hoke et al. 2007; Houston et al., 2008, Evenstar et al., 2009, Rech et al., 2006, 2010 among others). Crucial for the reconstruction of past environments and the understanding of the evolution of this region is the achievement of a reliable absolute chronology of the stratigraphic record. New radiometric and magnetostratigraphic data from the Quillagua Basin infill are presented here, which identifies alternating periods of active sedimentation and of long-lasting non-depositional hiatuses. A chronostratigraphic correlation with adjacent basins in the Atacama and Altiplano regions, as well as a comparison with the chronology of paleoclimatic and paleoceanographic changes at higher southern latitudes was carried out in order to assess the contribution of climatic forcing to the sedimentary record of the Atacama region.

2. Methods

A total of fourteen tephra layers from 10 sections in the basin center and the eastern basin margin were dated by $^{40}Ar/^{39}Ar$ step-heating. Sample preparations were carried out at the Petrology Laboratory of the University of Barcelona. Biotite and feldspar crystals were hand-picked from crushed and sieved splits and cleaned using an ultrasonic disintegrator. Separates were placed in aluminum trays and irradiation cans wrapped in 0.7 mm cadmium foil and neutron irradiated at the 5-MW reactor of the Helmholtz-Zentrum Geesthacht (HZG).

Age determinations were carried out by laser $^{40}Ar/^{39}Ar$ step-heating at the Helmholtz Centre for Ocean Research Kiel (GEOMAR). After purification the gas samples were analyzed using a MAP 216 series noble gas mass spectrometer. Raw mass spectrometer peaks were corrected for mass discrimination, background and blank values (measured every fifth analysis). The neutron flux was monitored using Taylor Creek

Rhyolite Sanidine (TCR-2: 27.87 ± 0.04 Ma; Lanphere and Dalrymple, 2000). Corrections for interfering neutron reactions on Ca and K are based on analyses of optical grade CaF_2 and high-purity K_2SO_4 salt crystals that were irradiated together with the samples. Alteration states were monitored according to Baksi (2007).

A total of 196 oriented paleomagnetic samples were drilled in situ at evenly distributed stratigraphic intervals of 2 meters approximately, avoiding the coarser grained intervals. All samples were routinely stepwise demagnetized using a shielded furnace and the remanent magnetization measured in a three-axis superconducting magnetometer hosted at the Paleomagnetic Laboratory of the University of Barcelona and CSIC. Complete demagnetization often required >10 demagnetization steps up to peak temperatures of 600ºC, while demagnetization curves revealed unblocking temperatures preferentially ranging between 500 and 600ºC. The high average NRM and the steep remanence decay at temperatures below 600ºC was related to the abundance of magnetite of volcanic source, either as fallout contribution from active volcanoes or reworked from older eruptions.

Visual inspection of the demagnetization diagrams (Supplementary Fig. 1) allowed the identification of a northerly up viscous component which parallels the present day field and demagnetizes at temperatures below 300ºC. A Characteristic Remanent Magnetization (ChRM) is identified in the temperature interval ranging from 300ºC to 600 ºC, with a relatively high average intensity of 6.78 mA/m. The direction of the ChRM component was calculated by means of principal component analysis in 155 samples (80% of the total demagnetized samples). Virtual Geomagnetic Pole (VGP) latitudes were calculated for each paleomagnetic direction and a polarity interpretation was derived from each sample (Supplementary Figure 2). Normal and Reversed polarity magnetozones are indicated in the polarity logs as black and white intervals respectively. Single-site magnetozones are indicated as half-width polarity intervals in the polarity log (Supplementary Figure 2), but not considered sufficiently reliable, and not taken into account for correlation purposes.

A feasible correlation of the local magnetostratigraphy of Quillagua with the Geomagnetic Polarity Time Scale (Gradstein et al., 2004, Figure 2) is put forward on the basis of the several $^{40}Ar/^{39}Ar$ ages obtained from tephra layers interbedded within the sequence (Table 1).

3. Quillagua and Calama basins records

The Quillagua Basin (~21°-22º40'ºS, 800-2000 masl.) is a north-south oriented basin located in the southern part of the Central Depression or Pampa del Tamarugal, between the Coastal Range and the

Precordillera (Fig. 1), presently draining to the Pacific Ocean through the Loa River Canyon (Fig. 1). From late Miocene to Pleistocene, this basin was internally drained, leading to the accumulation of nearly 200 meters of alluvial sediments, interbedded with three lacustrine units and some tephra layers in the central part of the basin (Jensen, 1992; Sáez et al., 1999; Pueyo et al., 2001) (Fig. 2). Well developed fluvial fan deposits in the eastern basin margin consist mainly of conglomerates that merge basinward into fine-grained sandstones and red mudstones, sourced from the Western Cordillera (i.e., Arcas Fan deposits, Kiefer et al., 1997). Minor fluvial sandstone and gravel contributions from the south corresponding to paleo-Loa River deposits also occur. From old to young, the lacustrine units consist of gypsum-anhydrite deposits (Hilaricos Unit), diatomite, marls, silty limestone, gravelly sandstone and minor tufa deposits (Quillagua Fm) and halite (Soledad Fm).

Deposits of Quillagua Fm are 130 m-thick and paraconformably overlie alluvial red beds in Qda. Temblor (site 3), whereas in Puente Posada (site 4) these deposits rest unconformably over similar alluvial facies (Figs. 1 and 2). Stratigraphy, sedimentology and paleogeography of this unit have been extensively analyzed previously elsewhere (Sáez et al., 1999; Bao et al., 1999; Pisera and Sáez, 2003) and its description is beyond the scope of this contribution. In the inner-central basin zone, between Cerro Mogote and Qda. Temblor sites, Quillagua Fm deposits are organized in two cycles of expansion and retraction of lacustrine facies (4th-order cycles), each of them arranged in ~20 5th-order transgressive-regressive lacustrine cycles (Fig. 2) (Sáez et al., 1999; Bao et al., 1999). The halite sequence of the Soledad Fm is 100 m-thick, shows physical continuity with saline deposits of the Salar Grande and unconformably overlies Hilaricos unit in the sector of Lomas de la Sal (Pueyo et al., 2001).

The Late-Pleistocene Soledad Formation was deposited from water contributions of the ancient Loa River that currently collect water contribution from extense high altitude zones located to the East of the Atacama Desert and yields an average permanent flow of 2.43 m^3/s. Nevertheless, the spill of the Loa River into the Pacific Ocean resulted in a drop of ~ 1000 m of the base level that triggered the present entrenchment phase of the central areas in the basin, preventing further accumulation of extensive lacustrine deposits since water was not retained any longer in the basin.

Towards the eastern margin, the basin infill is up to a 600 hundred m-thick and consists of a syntectonic red bed sequence that encompasses alluvial deposits, dated from 24.0 to almost 5.8 Ma (Tomlinson et al., 2001; Hoke et al., 2007). So far, in the inner basin zone, only the lower and mid- intervals of the stratigraphic sequence have been dated. K/Ar on biotites, yield an age of 6.0 and 5.8 Ma for the Hilaricos and Quillagua deposits respectively (Sáez et al., 1999).

The Calama Basin (22°-23ºS, 2000-3000 masl.) is a depression situated between the Precordillera and the Western Cordillera (Fig. 1) and it is currently drained to the Pacific Ocean by the Loa River catchment (Fig. 1). The drainage communication between the Calama and Quillagua basins ranged from closed-restricted to open during their evolution, due to the likely development of tectonic thresholds (Sáez et al., 1999; May et al., 1999). Early Miocene to Recent alluvial systems spread from different source areas located around the basin margins. Basin sedimentation was not continuous but during some time intervals nearly 250 meters of alluvial and lacustrine sediments were accumulated at the central and southern sectors or the basin (Chiquinaputo, Opache, Chiu-Chiu Fms). Some tephra layers have been reported in these sequences (May et al. 1999, 2005; Blanco, 2008).

The Chiquinaputo Fm includes minor diatomite and carbonate tufa interbedding red alluvial deposits. In the southern basin sector this unit unconformably overlies Lasana or Jalquincha Fms deposits and it includes at its bottom an ignimbrite dated to 10.3/9.4Ma (Blanco, 2008) and another volcanic layer at the top dated to 7.82 Ma (Rech et al., 2010). The Opache Fm is composed by carbonate-cemented conglomerate and sandstone, limestone and diatomaceous marl that have been dated between 5.76 and 3.37 Ma thanks to two volcanic ash layers interbeded near the bottom and the top of the formation (May et al., 2005). The Chiu-Chiu Fm unconformably overlies folded strata of Opache Fm, includes diatomite and carbonate tufa interbedding clastic deposits. This unit has been imprecisely dated between 3.37 Ma of the top of Opache Fm and 0.45 Ma of the overlying swampy fluvial deposits (Blanco 2008). Despite the reported differences in the dating of the diverse sedimentary units, several authors have reported long sedimentary gaps between Jalquincha/Lasana and Opache Fms and between Opache and Chiu-Chiu Fms (May et al, 2005; Blanco, 2008; Rech et al 2010).

4. Results

Results of the $^{40}Ar/^{39}Ar$ laser step-heating analyses are listed in Table 1. The tephra layers studied from the basin center and the eastern alluvial basin margins yield ages that cluster into three distinct groups: from 7.8 to 8.8 Ma (Hilaricos Fm), from 5. 0 to 5.6 Ma (Quillagua Fm), and Late Pleistocene (0.1 to 0.2 Ma; Soledad Fm).

The magnetostratigraphic study carried in the Quillagua Basin which complements the isotope geochronology, providing a detailed chronostratigraphic framework for the basin infill. Three partially overlapping sections in the basin center were sampled for this purpose, and 155 samples were stepwise demagnetized in a paleomagnetic laboratory (see Supplementary Information, Fig. 2). The overall results

yielded a consistent pattern of reversals, with a number of samples/magnetozone sufficient to ensure completeness of the magnetostratigraphic record. The derived magnetostratigraphy consists, however, of a remarkably low number of reversals compared to the age range presumed from radiometric dating. Given these radioisotopic constraints, the low number of reversals recorded in the sequence indicates that very significant sedimentary gaps must exist, so that periods of sedimentation in the basin represent less than half of the total time span. On the basis of the available radiometric constraints, a correlation with the geomagnetic polarity time scale is proposed (Fig. 2), where two sedimentary hiatuses on the order of millions years each are inferred.

The comparison of the Late Cenozoic stratigraphic records of Quillagua and Calama basins shows significant parallelism, in terms of chronology of depositional units, hiatuses, as well as sedimentation rates. Thus, a very low, long-term sedimentation rate (~ 2.0 cm/kyr) is recorded in the inner Quillagua Basin. Net sediment accumulation only occurred during three relatively short periods lasting a total of 2.9 Ma to record the 185 m-thick sequence. Non-depositional intervals spanned 70% of the last 10 Ma. From published stratigraphic data from the central parts of the Calama Basin (Tomlinson et al., 2001; Blanco, 2008; Blanco and Tomlinson, 2009) the sedimentation rate can be calculate in ~ 2.3 cm/kyr. Both basins show a relative synchronicity in the evolution of lacustrine and alluvial environments as well (Fig. 3), suggesting that a major leading regional factor controlled the overall depositional history.

5. Discussion: Climate forcing

Tectonic and geomorphologic factors have been regarded as determinant controls for the sedimentation in the Central Depression (Naranjo and Paskoff, 1982; Houston et al., 2008). However, the recurrent expansion of neogene lacustrine units in the internally drained Quillagua Basin can be well regarded as climatically controlled. The fairly good fit between major non-sedimentary and sedimentary periods between Quillagua and Calama basins and between other records in the region (i.e. upper Salar Grande and Salar de Atacama basins), lead us to propose that the major forcing factor in the Atacama region was the oscillation from hyperarid to less arid climatic conditions. The hyperarid climate conditions correlate with hiatuses in the central basin areas as a result of lack of sediment production; and the less arid conditions to low alluvial and lacustrine sedimentation rates.

Our chronology is a step towards recognizing the importance of climate forcing in the fluvial-lacustrine records of the Quillagua Basin (Saéz et al., 1999). Small meter-scale transgressive-regressive lacustrine sequences have an average duration of 20 kyr, thus most likely representing precession cycles. These are organized into lower order sequences with a mean duration close to the 400-kyr eccentricity period (Fig. 3).

At a larger scale, the sediments of the inner or distal zones of the Quillagua and Calama basins are organized into units separated by long-lasting sedimentary gaps, these features interpreted as the response to the long-term oscillations of climate, shifting from arid to hyperarid conditions. The presence of unconformity surfaces and abrupt changes of lithology, both matching with the sedimentary hiatuses, strengthen the interpretation of the existence of these long periods of no sedimentation in the Quillagua Basin (Fig. 2).

The new integrated chronostratigraphy of the Quillagua and Calama basins allows a correlation with records of global and regional climate change found to have an effect on the continental paleoenvironments of South America. The growth of the Western Antarctic ice-sheet (Zachos et al., 2001), coeval to times of full glaciation in Patagonia (Rabassa et al., 2005), as well as cold seawater paleotemperatures on the Peru coast (Abe et al., 2006; Tiedemann and Mix, 2007; Amiot et al., 2008) have been recorded between 7 and 5.5 Ma. Seawater cooling was related to the intensification of the Humboldt Current, with equatorward advection and upwelling of cold subpolar waters in connection with glaciation in Antarctica and the oceanic thermocline shallowing (Dekens et al., 2007). Cold water along the western border of subtropical South America strengthened the regional anticyclone and triggered hyperarid phase 1 that resulted in Gap 1 (Fig. 3). Conversely, during the subsequent early Pliocene warm period coeval with ice sheet retreat in Antarctica (Haywood et al., 2008) and in Patagonia (Rabassa et al., 2005) the Humboldt current weakened and the temperature of upwelled coastal water along the Chile-Peru coastal region was warmer from c. 4.6-3.1 Ma due to the oceanic thermocline deepening, as expected during permanent El Niño-like conditions (Dekens et al., 2007). Warm seawater over the adjacent southeast Pacific Ocean weakened the subtropical anticyclone and triggered higher precipitation (Garreaud et al., 2010) that resulted in the deposition of alluvial-lacustrine sequences (Quillagua and Opache Fms) in the central basin zones (Fig. 2). Renewed water cooling linked to the spreading of the Antarctic Ice sheets to their present polar cold stage between 3 and 2.5 Ma (Naish et al., 2008; Fig. 3) and the renewed cold water upwelling in the tropical-subtropical eastern Pacific embracing the Pliocene/Pleistocene transition (Wara et al., 2005) triggered the currently ongoing second hyperarid phase in Atacama that generated Gap 2.

The Soledad Fm, together with other coeval lacustrine deposits (Chiu-Chiu Fm in Calama Basin; upper halite deposits at the Salar Grande and Salar de Atacama Basin; Pueyo et al., 2001; Bobst et al., 2001) record basin evolution stages with higher water contribution that modulated the overall hyperarid Phase 2. Both climatic and geomorphic factors are proposed to explain this water contribution that triggered the sedimentation of Soledad Fm in the Quillagua basin before it was opened to the Pacific Ocean. From a

climatic point of view, increase of precipitation in the higher altitude regions located to the East of the Atacama region seems to be linked to the prevailing La Niña-like conditions (Betancourt et al.,2000) and could afford for episodes of larger water income into the lower altitude zones. From a geomorphic point of view the eastward enlargement of the Loa river catchment would have triggered and enabled a larger water contribution from the higher altitude catchments located to the East of Atacama Desert.

The late Pleistocene lacustrine episodes in the Atacama region (Soledad Fm., Salar Grande, Chiu-Chiu, Salar de Atacama) were coeval with a deep-lake, moist stage cycle (Ouki phase) that occurred between 120 and 98 ka in the Andean Altiplano Poopo Basin (Placzek et al., 2006). Moreover, Nester et al. (2007) and Latorre et al. (2006) have reported younger late Pleistocene water discharge episodes in the Central Depression, these also coeval with spreading and deepening of lakes in the Altiplano. These water contribution increases have been attributed to intensification of the SASM in its turn related to pronounced equatorial sea surface temperature gradients under persistent La Niña-like conditions at different (i.e. centennial to millennial) time scales (Betancourt et al., 2000). Rech et al. (2006) suggested that these conditions may have occasionally increased water contribution into the Atacama region from its eastern higher altitude margins even since Middle Miocene.

We conclude that million year-scale, sedimentary hiatuses developed in the Atacama region were coeval to (1) growth of ice volume in Antarctica and Patagonian glaciers; and (2) cold water periods in the neighboring ocean, as a consequence of the reinforcement of the Humboldt Current and cold water upwelling. Climate forcing is thus proposed for the Late Neogene stratigraphic record in the Atacama region, where cooling stages sustained extreme hyperarid conditions, these accounting for the occurrence of prolonged sedimentary gaps in the central depressions (Fig. 3). The development of the extensive late Pleistocene saline lacustrine deposits in the Quillagua basin under the ongoing hyperarid conditions resulted from a combination of increasing precipitation in the higher altitude catchments to the East of Atacama Desert and of water transfer to the low lying basins enhanced by the likely eastward enlargement of the Loa river catchment.

Acknowledgments

This research was funded by Spanish Government projects: PB94-0901, CGL2004-00780, CGL2007-66431-C02-02/BTE, CGL2007-60932/BTE and CGL2010-17479; and by Generalitat de Catalunya through Research Institute GEOMODELS and the Research Group of “Geodinàmica i Anàlisi de Conques” (2009 GGR 1198). Thanks are due to A. Carroll, C. Connors and E. Gierlowski by the critical reading of an early

256 version of this paper. We are grateful to Teresa Jordan, Rene Garreaud , two anonymous reviewers and the
257 EPSL editor for their useful revisions and comments that enabled us to precise the paper content.

References

Abe, C., Yamamoto, M., Irino,T., 2006. Data report: organic carbon and biomarker variations, Sites 1237 and 1239. In Tiedemann, R., Mix, A.C., Blum, P. and Ruddiman, W.F. (Eds). Proceedings of the Ocean Drilling Program, Scientific Results, 202: College Station, TX (Ocean Drilling Program), 1-14.

Amiot, R., Göhlich, U.B., Lécuyer, C., de Muizon, C., Cappetta, H., Fourel, F., Héran, M-A., Martineau, F., 2008. Oxygen isotope compositions of phosphate from Middle Miocene-Early Pliocene marine vertebrates of Peru. Palaeogeography, Palaeoclimatology, Palaeoecology, 264, 85-92.

Baksi, A.K., 2007. A quantitative tool for detecting alteration in undisturbed rocks and minerals - I: Water, chemical weathering, and atmospheric argon, in: Foulger, G.R., Jurdy, D.M. (Eds), Plates, Plumes and Planetary Processes. Spec. Pap. Geol. Soc. Am. 430, 285-303.

Bao, R., Sáez, A., Servant-Vildary, S., Cabrera, L., 1999. Lake-level and salinity reconstruction from diatom analyses in Quillagua Formation (Late Neogene, Central Andean Forearc, Northern Chile). Palaeogeography, Palaeoclimatology, Palaeoecology 153, 309-335.

Blanco, N., 2008. Estratigrafía y evolución tectono-sedimentaria de la cuenca cenozoica de Calama (Chile, 22°S). M.S. Thesis. University of Barcelona. 68 p. (Spanish).

Blanco, N., Tomlinson, A., 2009. Carta Chiu Chiu, Región de Antofagasta. Servicio Nacional de Geología y Minería, Carta Geológica de Chile, Series Basic Geology. 26 p., Scale 1:50.000. Santiago.

Betancourt, J.L., Latorre, C., Rech, J.A., Quade, J., Rylander, K.A., 2000. A 22,000-year record of monsoonal precipitation from Northern Chile's Atacama Desert. Science 289, 1542-1546.

Bobst, A.L., Lowernstein, T.K., Jordan, T. E., Godfrey, L.V., The-Lung Ku, and Shangde Luo, 2001. A 106 Ka paleoclimate record from drill core of the Salar de Atacama, northern Chile. Palaeogeography, Palaeoclimatology, Palaeoecology 173, 21-42.

Dekens, P.S., Ravelo, A.C., McCarthy, M.D., 2007. Warm upwelling regions in the Pliocene warm period. Palaeceanography 22, PA3211.

Dunai, T.J., Gonzalez, G.A., Juez-Larré, J., 2005. Oligocene–Miocene age of aridity in the Atacama Desert revealed by exposure dating of erosion sensitive landforms. Geology 33, 321-324.

Garreaud, R.D., Molina, A., and Farias, M., 2010. Andean uplift, ocean cooling and Atacama hyperaridity. A climate modeling perspective. Earth and Planetary Science Letters 292, 39-50.

Gaupp, R., Kött, A., Wörner, G., 1999. Paleoclimatic implications of Mio-Pliocene sedimentation in the high-altitude intra-arc Lauca Basin of northern Chile. Palaeogeography, Palaeoclimatology, Palaeoecology 151, 79-100.

Gradstein, F.M., Ogg, J.G., Smith A., 2004. A Geologic Time Scale 2004. Cambridge University Press, Cambridge.

Harley, A.J., 2003. Andean uplift and climate change. Journal of the Geological Society of London 160, 7-10.

Hartley, A.J., Chong, G., 2002. Late Pliocene age for the Atacama Desert. Implications for the desertification of western South America. Geology 30, 43-46.

Haywood, A.M., Smellie, J. L., Ashworth, A. C., Cantrill, D.J., Florindo, F., Hambrey M. J., Hill, D., Hillenbrand, C., Hunter, S.J., Larter, R.D., Lear, C.H., Passchier, S., van de Wal, R., 2008. Middle Miocene to Pliocene History of Antarctica and the Southern Ocean. Developments in Earth & Environmental Sciences 8, 401-463.

Kiefer, E., Dörr, M.J., Ibbeken, H., Götze, H-J., 1997. Gravity-based mass balance of an alluvial fan giant: the Arcas Fan, Pampa del Tamarugal, Northern Chile. Revista Geológica de Chile 24, 165-185.

Hoke, G. D., Isacks, B.L., Jordan, T.E., Blanco, N., Tomlinson, A.J., Ramezani, J., 2007. Geomorphic evidence for post-10 Ma uplift of the western flank of the central Andes 18º30'-22ºS. Tectonics 26, TS5021.

Houston, J., Hart, D., Houston, A., 2008. Neogene sedimentary deformation in the Chilean forearc and implications for Andean basin development, seismicity and uplift. Journal of Geological Society, London 165, 291-306.

Jensen, A., 1992. Las cuencas aluvio-lacustres oligoceno-neógenas de la region de ante-arco de Chile Septentrional, entre los 19º y 23 º sur. Ph.D. Thesis, Universidad de Barcelona; Spain, 217 pp.

Lanphere, M.A., Dalrymple, G.B., 2000. First-principles calibration of 38Ar tracers: Implications for the ages of 40Ar/39Ar fluence monitors. U.S. Geological Survey Professional Paper 1621, 10 p.

Latorre, C., Betancourt, J.L., Arroyo, M.T.K. , 2006. Late Quaternary vegetation and climate history of a perennial river canyon in the Rio Salado basin (22 degrees S) of Northern Chile. Quaternary Research 65, 450-466.

Le Roux, J.P., 2012. A review of Tertiary climate changes in southern South America and the Antarctic Peninsula. Part 2: continental conditions. Sedimentary Geology 247–248, 21-38.

May, G., Hartley, A., Chong, G., Stuart, F., Turner, P., Kape, S., 2005. Eocene to Pleistocene lithostratigraphy, chonostratigraphy and tectono-sedimentary evolution of the Calama Basin, northern Chile. Revista Geológica de Chile 32, 33-58.

Naish, T., Carter, L. , Wolff, E., Pollard, D., Powell, R., 2008. Late Pliocene-Pleistocene Antarctic Climate Variability at Orbital and Suborbital Scale. Ice Sheet, Ocean and Atmospheric Interactions. Developments in Earth & Environmental Sciences 8, 465-529.

Naranjo, J.A., Paskoff, R.P., 1982. Estratigrafía de las unidades sedimentarias cenozoicas de la Cuenca del Río Loa en la Pampa del Tamarugal, Región de Antofagasta, Chile. Revista Geológica de Chile 15, 49-57.

Nester, P. L., Gayó, E., Latorre, C., Jordan, T. E., Blanco, N., 2007. Perennial stream discharge in the hyperarid Atacama Desert of northern Chile during the latest Pleistocene. Proceedings of the National Academy of Sciences 104, 19724-19729.

Pisera, A., Sáez, A., 2003.Paleoenvironmental significance of a new species of freshwater sponge from the Late Miocene Quillagua Formation (N Chile). Journal of South American Earth Sciences 15, 847–852.

Placzek, C., Quade, J., Patchett, P.J., 2006. Geochronology and stratigraphy of the late Pleistocene lake cycles on the southern Bolivian Altiplano. Implications for causes of tropical climate Change. GSA Bulletin 118, 515-532.

Pueyo, J.J., Chong, G., Jensen, A., 2001. Neogene evaporites in desert volcanic environments. Atacama Desert, northern Chile. Sedimentology 48, 1411-1431.

Rabassa, J., Coronato, A.M., Salemme, M., 2005. Chronology of the Late Cenozoic Patagonian glaciations and their correlation with biostratigraphic units of the Pampean region (Argentina). Journal of South American Earth Science 20, 81-103.

Rech, J.A., Currie, B., Michaslski, G., Cowan, A.M., 2006. Neogene climate change and uplift in the Atacama Deserts, Chile. Geology 34, 761-764.

Rech, J.A., Currie, B., Shullenberger, E.D., Dunagan, S.P., Jordan, T.E., Blanco, N., Tomlinson, A.J., Rowe. H.D., Houston, J., 2010. Evidence for the development of the Andean rain shadow from a Neogene isotopic record in the Atacama Desert, Chile. Earth and Planetary Science Letters 292, 371-382.

Sáez, A., Cabrera, L., Jensen, A., Chong, G., 1999. Late Neogene lacustrine record and paleogeography in the Quillagua-Llamara basin, Central Andean fore-arc (northern Chile). Palaeogeography, Palaeoclimatology, Palaeoecology 151, 5-37.

Tiedemann, R., Mix, A.C., 2007. 1. Leg 202 Synthesis: Southeast Pacific Paleoceanography. In Tiedemann, R., Mix, A.C., Blum, P. and Ruddiman, W.F. (Eds.). Proceedings of the Ocean Drilling Program, Scientific Results, 202: College Station, TX (Ocean Drilling Program), 1-56.

Tomlinson, A.J., Blanco, N., Maksaev, V., Dilles, J.H., Grunder, A.L., Ladino, M., 2001. Geología de la Precordillera Andina de Quebrada Blanca-Chuquicamata, Regiones I y II (20º30'-22º30'S). Santiago, Chile, Servicio Nacional de Geología y Minería, Informe Registrado IR-01-20, 2 volumes, 444 p.

Wara, M., Ravelo, A.C., Delaney, M.L., 2005. Permanent El Niño conditions during the Pliocene warm period. Science 309, 758-761.

Zachos, J., Pagani, M., Sloan, L., Thomas, E., Billups, K., 2001. Trends, rhythms and aberrations in global climate 65 Ma to present. Science 292, 686-693.

Figure and table captions

Figure 1. A. Location map showing present-day climatic zones of western South America; box shows area of map B. B. Geological sketch of the Quillagua and Calama basins. Red circles named (MAN, TAM, MO, TA, TE, ARC, CON, EN, ESQ, PUP) correspond to 10 sections in the central and the eastern margin of the Quillagua Basin where 14 tephra layers have been dated by $^{40}Ar/^{39}Ar$ (Table 1). Numbers in bold indicate sections in panel of Fig. 2. 1. Cerro Mogote section (MO), 2. Quebrada Tambillo section (TA), 3. Quebrada Temblor-Río Loa composite section (TE-FTE), 4. Puente Posada section (PUP). The main lacustrine units in Quillagua and the alluvial successions outcropping in both basins are mapped.

Figure 2. N-S stratigraphic cross section showing lithologic and paleomagnetic units of central areas of the Quillagua Basin and the diverse bounding unconformities and hiatuses. Blue line depicts changes in the lacustrine facies (Sáez et al., 1999) and represents higher order transgressive-regressive lacustrine sequences recording ~20 kyr precession cycles. Red line depicts lower order sequences recording ~400-kyr eccentricity cycles.

Figure 3. Correlation of sedimentation and non-sedimentation stages in the central part of the Quillagua Basin and the meridional-distal margin of Calama Basin. Antarctic climate events affecting South America, Patagonian glaciations and changes of upwelling water temperatures during last 10 Ma are included (Rabassa et al., 2005; Haywood et al., 2008: Naish et al, 2008; Abe et al., 2006; Tiedemann and Mix, 2007). The colors in the bar that represents upwelling water temperature are a qualitative indication of the overall trends of temperature change while the superimposed curve of temperature corresponding to the last 6 million years has been adapted from Abe et al., 2006. Eccentricity (E) and precession (P) cycles recorded during the late Miocene-early Pliocene depositional stage are shown. The short term episodes of water contribution from the higher altitude zones to the East of Atacama Desert and likely linked to the reinforcement of the South American Summer Monsoon during La Niña-like situation are also shown. 1. Artola ignimbrite at the top of Jalquinche Fm (10.3/9.4 Ma; Blanco, 2008), 2. Sifón ignimbrite interbedding Chiquinaputo Fm (7.82 Ma, Rech et al., 2010), 3. Near bottom of Opache Fm (5.76 Ma; May 2005), 4. Top Opache Fm (3.37 Ma; May et al., 2005), 5. Chiu-Chiu Fm (between 3.37 and 0.45 Ma; Blanco, 2005). 6. Lower outcropping Hilaricos Unit (paleomagnetic data, this study), 7. Near top Hilaricos Unit, 8.75 Ma (this study), 8. Top Hilaricos Unit (paleomagnetic data, this study), 9. Top of red distal Arcas deposits (paleomagnetic data, this study), 10. Bottom of Quillagua Fm (5.54/5.36 Ma, this study), 11. Eroded top of Quillagua Fm (paleomagnetic data, this study). 12. Near bottom of Soledad Fm (0.2-0.1 Ma, this study).

Table 1. $^{40}Ar/^{39}Ar$ date of sampled tephra layers from Quillagua Basin. Location, unit and tephra layer characteristics are also included. See map of figure 1 for section samples location.

Highlights

- Stratigraphic record in Atacama over the last 10 Ma includes two hiatuses
- The two hiatuses lasted 2 and 4 million years
- The hiatuses represent periods of hyperaridity in the region
- Gaps are synchronic with Antarctic glaciations and Humboldt C. enhancement
- South American Summer Monsoon modulated the hyperaridity trends.

Figure 1

Click here to download Figure: Fig. 1 Map EPSL.pdf

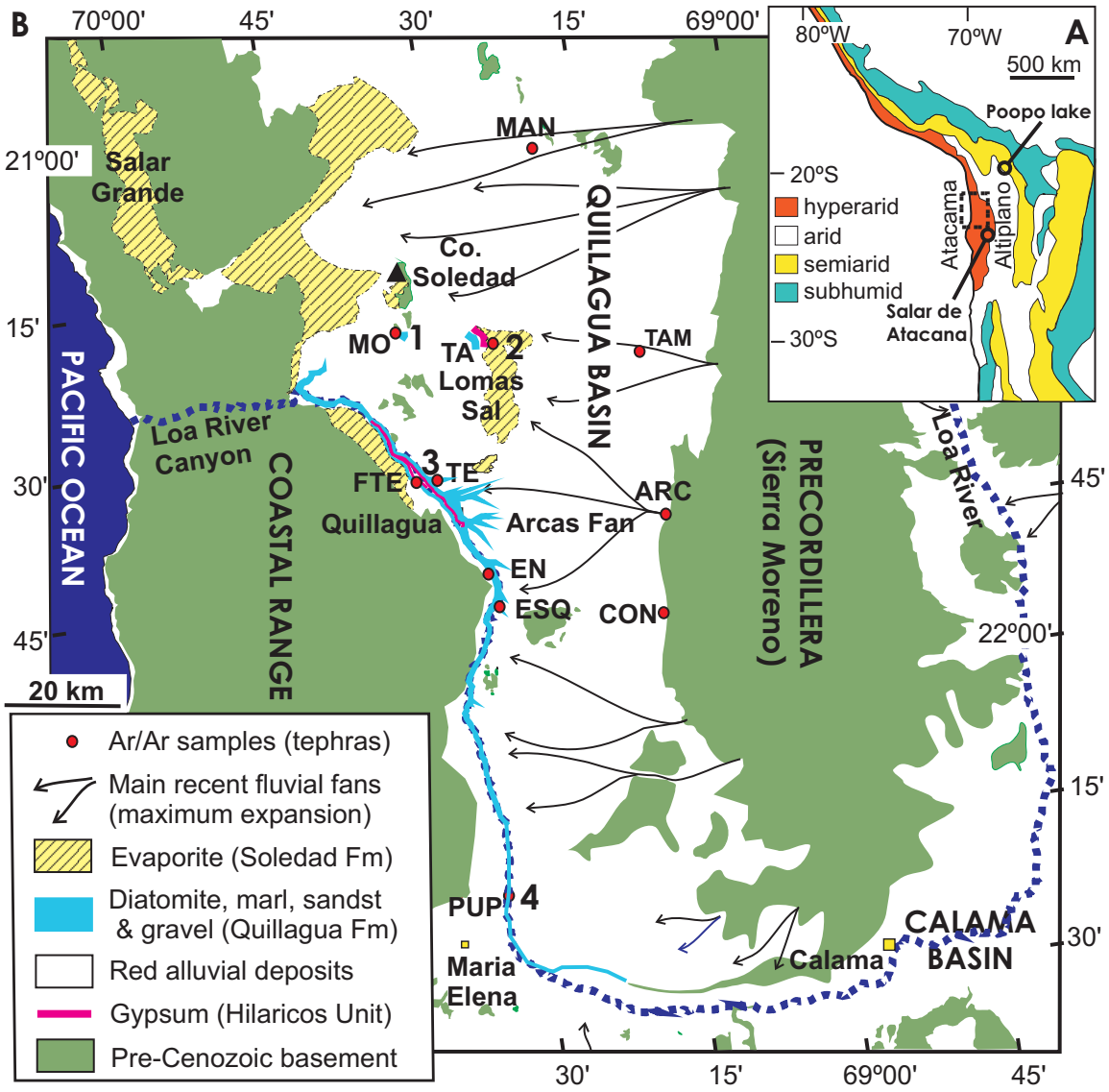

Figure 2

Click here to download Figure: Fig. 2 Panel EPSL.pdf

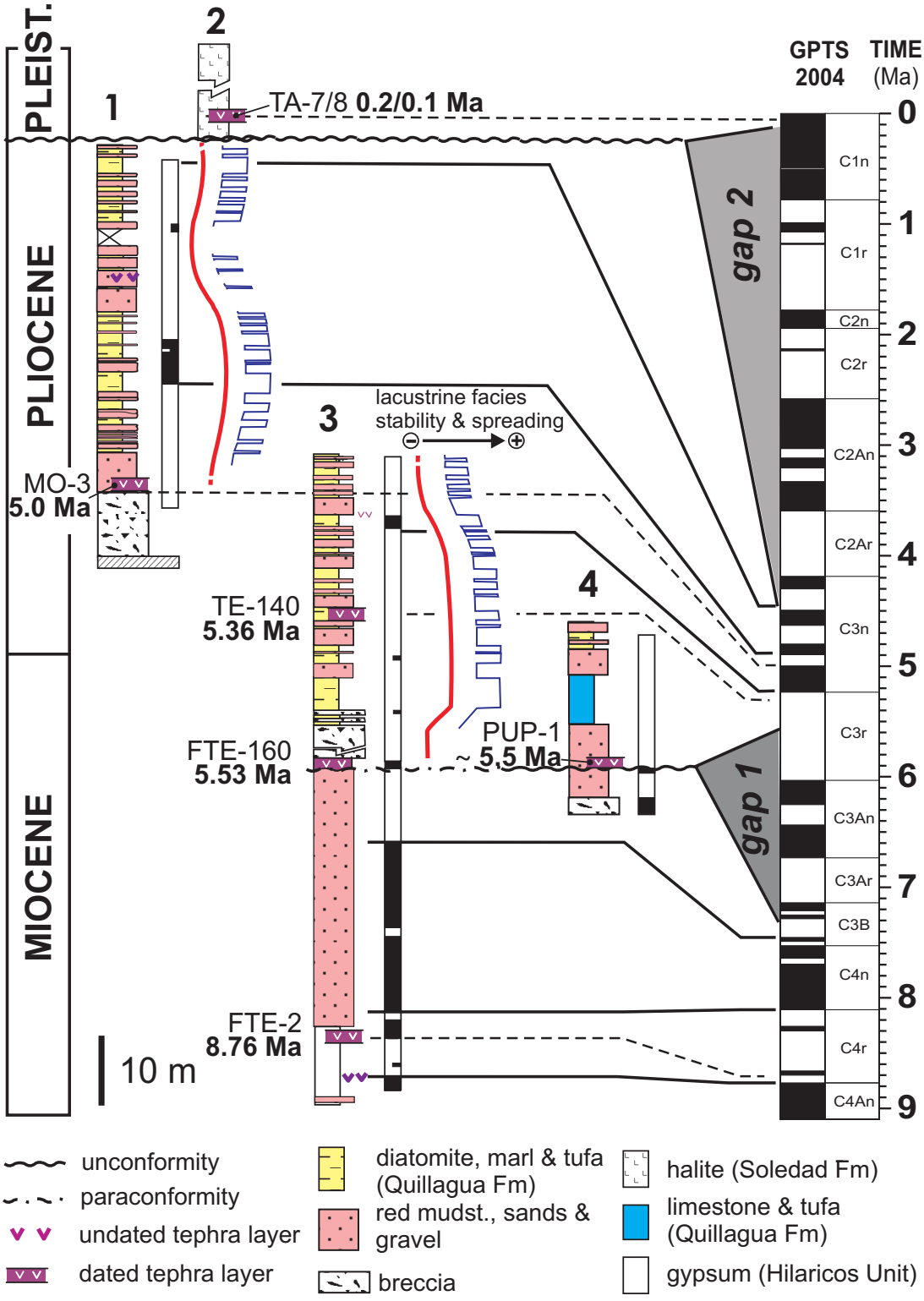

Figure 3

Click here to download Figure: Fig. 3 EPSL revised.pdf

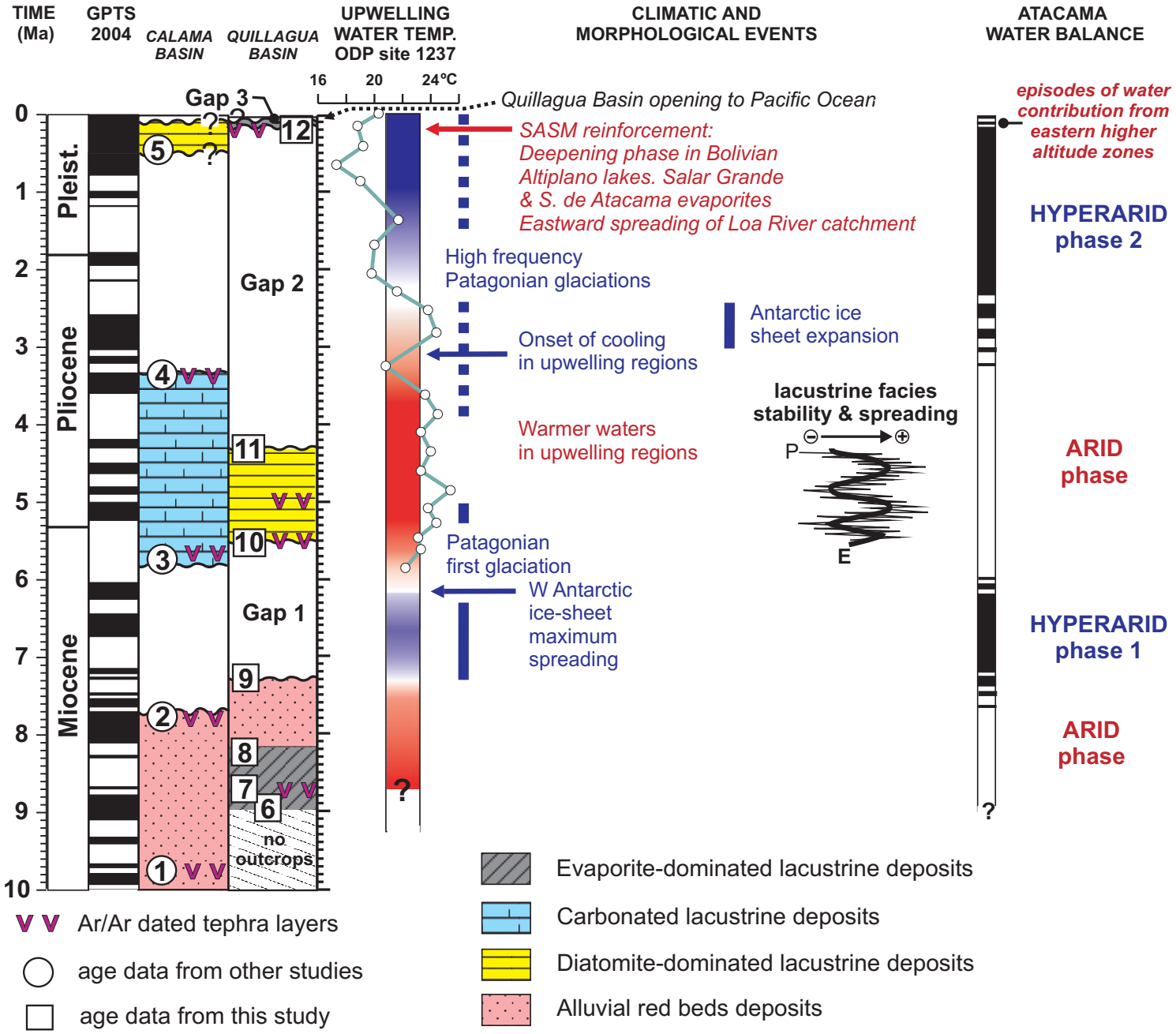

Table 1

Click here to download Table: Table 1 Ar-Ar date EPSL.pdf

Sample	Lab No.	Coordinates		Location, unit and tephra layer characteristics	Material	Type of data	Age (Ma)	±2σ	MSWD	Probability	$\%^{39}Ar$	Number of steps	Plateau steps alteration index
		Latit. S	Long. W										
TA8	TA8btsi	21°23'51"	69°25'10"	Co. Tambillo Alto in Lomas de la Sal. Lower Soledad Fm. Crusted layer between halite layers	Biotite	Plateau	0.21	±0.066	0,44	0.85	65.5	10 to 16 of 18	<0.001
TA7	TA7btsi	21°23'51"	69°25'10"	Co. Tambillo Alto in Lomas de la Sal. Lower Soledad Fm. 35 cm-thick layer between halite layers	Biotite	Plateau (low-prob.)	0.098	±0.042	3.0	0,02	52.1	9 to 13 of 14	<0.0005
ESQ1	ESQ1bts	21°49'01"	69°29'28"	Paso Borax of Loa river. Distal alluvial E Margin.Lenticular layer in channel 2.30 m-thick	Biotite	Plateau	0.151	±0.033	0.98	0.46	93	7 to 17 of 18	<0.0005
CON1	CON1bt2	21°51'16"	69°14'27"	Los Condores sector, E alluvial margin. Layer 50 cm-thick above a breccia	Biotite	Plateau (low-prob.)	0.181	±0.056	2.9	0.003	88.5	9 to 17 of 19	<0.0005
TE140	TE140fss	21°36'00"	69°33'07"	Qda. Temblor. Mid Quillagua Fm, 10 cm-thick between diatomites	Feldspar	Single step age	5.36	±0.05	-	-	60.4	step 19 of 19	0.00004
FTE160	FTE160bts	21°35'47"	69°35'01"	Western side Rio Loa, in front of Qda. Temblor. At the base of Quillagua Fm. Several layers, 5 to 7-m thick	Biotite	Plateau	5.535	±0.036	1.08	0.37	94.5	7 to 17 of 19	<0.001
MO29	MO29bts	21°21'08"	69°34'42"	Cerro Mogote. Mid Quillagua Fm, tabular layer 30 cm thick	Biotite	All steps weighted mean	5.55	±0.2	6.6	0,000	100	1 to 20 of 20	0.002-0.4 (strongly altered)
MO3	MO3bts	21°21'5.81	69°34'39"	Cerro Mogote. Lower Quillagua Fm., tabuler layer 20 cm thick.	Biotite	Plateau	5.046	±0.034	2.2	0.063	55.9	12 to 16 of 20	<0.0005
PUP1	PUP1bts	22°16'39"	69°33'37"	Puente Posada. Quillagua Fm base. Lenticular layer 1 m-thick in a chanel between red mudstones	Biotite	Plateau (low-prob.)	5.66	±0.12	3.4	0.009	58.3	13 to 17 of 20	<0.0005
TAM2	TAM2bts	21°26'41"	69°10'59"	Qda. Tambillo. E Alluvial margin.	Biotite	Plateau	5.303	±0.043	0.81	0.58	89.1	10 to 17 of 20	<0.001
ARC2	ARC2bt2	21°42'59"	69°10'59"	Qda. Arcas, E Alluvial margin. Layer, 3 m thick, between conglomerates. 5 m below ARC3	Biotite	Plateau	5.509	±0.032	1.9	0.088	65	11 to 16 of 18	<0.001
ARC3	ARC3bts	21°42'59"	69°10'59"	Qda. Arcas, E Alluvial margin. Lenticular layer, 5.5 m max. thick between conglomerates	Biotite	Plateau	5.369	±0.031	1.8	0.095	74.1	11 to 17 of 20	<0.001
MAN4	MAN4bts	21°05'47"	69°16'03"	Qda. Mani. E alluvial margin. Layer 20 cm-thick between conglomerates, near top of the sequence	Biotite	Plateau	8.76	±0.05	1.4	0.18	77.2	7 to 18 of 18	<0.001
FTE2	FTE2bts	21°35'47"	69°35'01"	Western side Rio Loa, in front of Qda. Temblor. Hilaricos Unit, top	Biotite	Plateau	8.756	±0.046	1.8	0.09	71.1	11 to 17 of 20	<0.001

Plateau criteria: at $^{40}Ar/^{36}Ar_i$=295.5; >3 consecutive steps identical within 2Sigma, 95% confidence level, probablity>5%; ^{39}Ar fraction >50%. Biotite alteration index = $^{36}Ar/^{39}Ar$ corrected for $^{36}Ar_{Ca}$ and normalized to J = 0.01 and K = 8% (<0.0005 for fresh biotite step-heating plateau steps). Feldspar (plagioclase) alteration index = $^{36}Ar/^{37}Ar$ corrected for $^{36}Ar_{Ca}$ and normalized to J = 0.01 (<0.00006 for fresh plagioclase step-heating plateau steps) (Baksi, 2007).

Supplementary mat Fig. 1

Click here to download Supplementary material for on-line publication only: Suppl Figure 1 Zijd-plots EPSL_LR.pdf

Supplementary mat. Fig. 2

Click here to download Supplementary material for on-line publication only: Suppl Figure 2 logs_EPSL.pdf